

# Quantification of Artifacts and Image Distortions in 1.5 Tesla Magnetic Resonance Images of a Commercial Multi-Channel Vaginal Cylinder Brachytherapy Applicator Set

Abolfazl Kanani (MSc)<sup>1</sup>, Ali Fatemi-Ardakani (PhD)<sup>2,3,4</sup>, Amir M. Owrangi (PhD)<sup>5</sup>, Mehran Yazdi (PhD)<sup>6</sup>, Hadi Baghbani (BSc)<sup>7</sup>, Mohammad Amin Mosleh-Shirazi (PhD)<sup>1,8\*</sup>

## ABSTRACT

**Background:** The BEBIG Portio multi-channel applicator provides better target dose coverage and sparing organs-at-risk compared to a single-channel cylinder. However, artifacts and distortions of Portio in magnetic resonance images (MRI) have not yet been reported.

**Objective:** We aimed to quantify the artifacts and distortions in its 1.5-Tesla MR images before clinical use.

**Material and Methods:** In this experimental study, we employed a gelatin-filled phantom to conduct our measurements. T2-weighted (T2W) images were examined for artifacts and distortions. Computed tomography (CT) images were used as a reference to assess image distortions. Artifact severity was measured by recording the full-width-at-half-maximum (FWHM) image pixel values at various positions along the length of the applicator/channels. CT and MRI-based applicator reconstruction accuracy were then compared, and signal-to-noise ratio (SNR) and contrast were also determined for the applicator images.

**Results:** The applicator distortion level for the Portio applicator was less than the image spatial resolution ( $0.5 \pm 0.5$  pixels). The average FWHM for the tandem applicator images was  $5.23 \pm 0.39$  mm, while it was  $3.21 \pm 0.37$  mm for all channels (compared to their actual diameters of 5.0 mm and 3.0 mm, respectively). The average applicator reconstruction difference between CT and MR images was  $0.75 \pm 0.30$  mm overall source dwell positions. The image SNR and contrast were both acceptable.

**Conclusion:** These findings indicate that the Portio applicator has a satisfactory low level of artifacts and image distortions in 1.5-Tesla, T2W images. It may, therefore, be a promising option for MRI-guided multi-channel vaginal brachytherapy.

**Citation:** Kanani A, Fatemi-Ardakani A, Owrangi AM, Yazdi M, Baghbani H, Mosleh-Shirazi MA. Quantification of Artifacts and Image Distortions in 1.5 Tesla Magnetic Resonance Images of a Commercial Multi-Channel Vaginal Cylinder Brachytherapy Applicator Set. *J Biomed Phys Eng.* 2023;13(6):523-534. doi: 10.31661/jbpe.v010.2309-1665.

## Keywords

Magnetic Resonance Imaging; Radiotherapy; Brachytherapy; Portio Applicator; Image Processing; Gynecological; Endometrial Cancer

## Introduction

Endometrial cancer ranks as the sixth most common cancer in women, with over 417,000 new cases reported in 2020 [1]. A common treatment approach involves postoperative vaginal brachytherapy (BT) with or without external beam radiation therapy

<sup>1</sup>Ionizing and Non-Ionizing Radiation Protection Research Center (INIR-PRC), School of Paramedical Sciences, Shiraz University of Medical Sciences, Shiraz, Iran

<sup>2</sup>Department of Physics, Jackson State University (JSU), Jackson, Mississippi, USA

<sup>3</sup>SpinTecx, Jackson, Mississippi, USA

<sup>4</sup>Department of Radiation Oncology, Community Health Systems (CHS) Cancer Network, Jackson, Mississippi, USA

<sup>5</sup>Department of Radiation Oncology, UT Southwestern Medical Center, 2280 Inwood Rd, EC2.242, Dallas, TX 75235, USA

<sup>6</sup>Signal and Image Processing Lab (SIPL), School of Electrical and Computer Eng, Shiraz University, Shiraz, Iran

<sup>7</sup>Department of Radiology, Namazi Hospital, Shiraz University of Medical Sciences, Shiraz, Iran

<sup>8</sup>Physics Unit, Department of Radio-Oncology, School of Medicine, Shiraz University of Medical Sciences, Shiraz, Iran

\*Corresponding author: Mohammad Amin Mosleh-Shirazi  
Physics Unit, Department of Radio-Oncology, School of Medicine, Shiraz University of Medical Sciences, Shiraz, Iran  
E-mail: amosleh@sums.ac.ir

Received: 18 September 2023

Accepted: 8 October 2023

(EBRT). Studies like PORTEC-2 have shown that vaginal cuff brachytherapy may offer advantages over EBRT, including reduced gastrointestinal and genitourinary toxicities and improved quality of life [2-4].

Significant improvements have been made in recent years with the implementation of volumetric imaging for BT treatment planning [5]. While earlier recommendations primarily focused on standardizing magnetic resonance imaging (MRI)-based planning for cervical cancer [6, 7], leading organizations like the American Brachytherapy Society (ABS), Groupe Européen de Curiethérapie—European Society for Radiotherapy & Oncology (GEC-ESTRO), and Canadian Brachytherapy Group (CBG) now emphasize the importance of 3D imaging, especially MRI, for endometrial/cervical vaginal recurrences [8, 9]. This shift highlights the need for careful commissioning of applicators to ensure safe and effective BT treatment planning using MRI. This includes assessing artifacts and distortions in a phantom environment before clinical use [10, 11].

Several cylindrical vaginal applicators of different lengths and diameters are now available commercially. Single-channel vaginal cylinder (SCVC) applicators are commonly used for superficial lesions, providing symmetrical dose distribution [12]. Multi-channel vaginal cylinder (MCVC) applicators have recently gained accessibility and popularity, featuring six to seven additional channels concentrically positioned around the central channel. MCVCs offer improved target dose coverage and better sparing of the uninvolved vaginas and organs at risk compared to SCVCs [13]. Karthik et al. reported the utilization of MCVC CT-based planning for early-stage endometrial cancer without compromising outcomes [14]. In a previous research, Owrangi et al. reported the clinical use of MRI-guided SCVC brachytherapy [15].

One of the latest commercialized MCVC applicators is the CT/MR Portio applicator

by Eckert & Ziegler BEBIG GmbH, Berlin, Germany. It can be used to treat the vaginal cuff, vaginal vault, cervix, and endometrium. Although this applicator is MR conditional, it can induce distortions and artifacts in images. To the best of our knowledge, an assessment of the susceptibility artifacts and distortions caused by MCVCs, and in particular the Portio applicator, has not been published yet. This is the first study describing this new Portio applicator.

The main goal of the current study is, therefore, to investigate the magnitudes of artifacts and image distortions in 1.5 T MR in-phantom images of the Portio applicator, utilizing custom-made tools for this purpose. Additionally, we assessed the feasibility of unaided applicator reconstruction (i.e., without using MRI contrast medium), which has been attempted in some previous research studies by inserting in-house MRI markers into the applicator to enhance visualization of the applicator tip [15-17].

## Material and Methods

### Applicator

In this experimental study, the Portio applicator was evaluated. It consists of a vaginal cylinder manufactured from PEEK plastic, featuring a central hole to accommodate an intrauterine (tandem) tube and six additional channels arranged concentrically around it for channels (Figure 1(a)). It is important to note that these closed-ended peripheral holes are contained within the plastic cylinder and are not intended for interstitial channel insertions. The cylinders are available in different diameters (25 mm and 30 mm). This study utilized a straight titanium intrauterine tube with a 5 mm diameter, a 30 mm diameter cylinder, and six 3 mm diameter plastic channels. To evaluate the individual contributions of the tandem to artifacts and image distortions, the tandem was positioned further than typical clinical scenarios, and as a result, the optional cap for

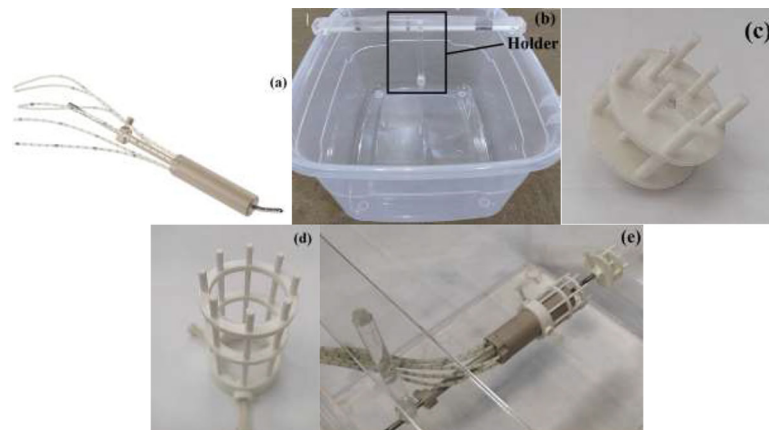


**Figure 1:** (a) The Portio applicator, (b) the magnetic resonance imaging (MRI)-compatible plastic phantom with a custom-made holder for suspending the applicator, (c, d) the fiducial markers for investigating distortion regarding the intrauterine tube and the channels, respectively, and (e) the assembly of the Portio applicator, the holder and the two fiducial sets.

the cylinder was not used.

### Phantom

The applicator was immersed in gelatin (13% volume) within a 29 L ( $46 \times 25 \times 25$  cm<sup>3</sup>) MRI-compatible plastic container using a customized holder (Figure 1(b)). The applicator was mounted in the same orientation concerning the main magnetic field as during treatment. The applicator was suspended about 8 cm away from the phantom's side to minimize potential distortions induced by the phantom material.

We employed two previously developed fiducial markers [18] to evaluate image distortion (spatial shift) induced by the tandem and channels. The first set comprised eight acrylonitrile butadiene styrene (ABS) rods, mounted on circular plates. We used two groups of rods, one having a 3 mm diameter and 10 mm center-to-center distance from the tandem (group 1) and the other with a 4 mm diameter and 17 mm center-to-center distance from the tandem (group 2) (as shown in Figure 1(c)). This set was tightly fitted over the tandem by a plastic screw. The spatial shift induced by the tandem was quantified by measuring the difference in distance between the tandem and fiducials in both CT and MR images. The sec-

ond fiducial set consisted of a central hole of 30 mm and eight ABS rods with a 3 mm diameter, separated by 45 degrees (Figure 1(d)). This set was also attached to the cylinder with plastic screws. The spatial shift induced by the channels and the cylinder was quantified by comparing the fiducials' position with that of the channels in both CT and MR images. Figure 1(e) shows the Portio assembled configuration with the fiducial set.

### MR and CT Imaging

MR scans were conducted using a standard-bore 1.5 T Ingenia MR scanner (Philips Medical Systems, Cleveland, OH, USA) with a body coil. Images were acquired in three planes: para-axial, with slices oriented perpendicular to the long axis of the tandem/cylinder; para-sagittal; and para-coronal, with cuts parallel to the long axis of the tandem. According to the Groupe Européen de Curiethérapie (GEC-ESTRO) and the American Association of Physicists in Medicine (AAPM) task group (TG) report 303 [19, 20], T2-weighted (T2W) fast spin-echo (FSE) sequence is the required sequence for gynecology (GYN) BT. Therefore, all analyses were performed on a 2D T2-weighted sequence with the following parameters: repetition time (TR)=3848

ms; echo time (TE)=90 ms; echo-train length (ETL)=30; voxel dimension= $0.45 \times 0.45 \times 2$  mm<sup>3</sup> with no slice gaps; number of excitations (NEX)=2. Fat Sat pulse was not applied. A 2D image distortion correction algorithm provided by the vendor was utilized for all MR images. Both MR images with and without the applicator were acquired.

CT scans were generated using a 20-slice Siemens SOMATOM Definition AS (Siemens Healthcare, Forchheim, Germany) scanner. Scan parameters included collimation of  $192 \times 0.6$ , tube voltage of 120 kVp, pitch of 0.6, reference mAs of 343, voxel dimension= $0.625 \times 0.625 \times 2$  mm<sup>3</sup>, and reconstruction with a convolution kernel of B30.

## Quantification of Applicator Distortion

The assessment focused solely on distortions induced by the Portio applicator, not system-specific distortions [10, 20]. A different image was created as explained in the previous section. The CT dataset was chosen as the reference. The image displays window-level values for the CT were adjusted until the dimensions of the tandem/channels matched their known actual physical dimensions. The differences between the tandem and eight markers shown in Figure 1(c) were measured at two locations (distal and medial in Figure 2(a)) in both CT and MR images (Figure 2(b)). All measurements were performed using the measure-

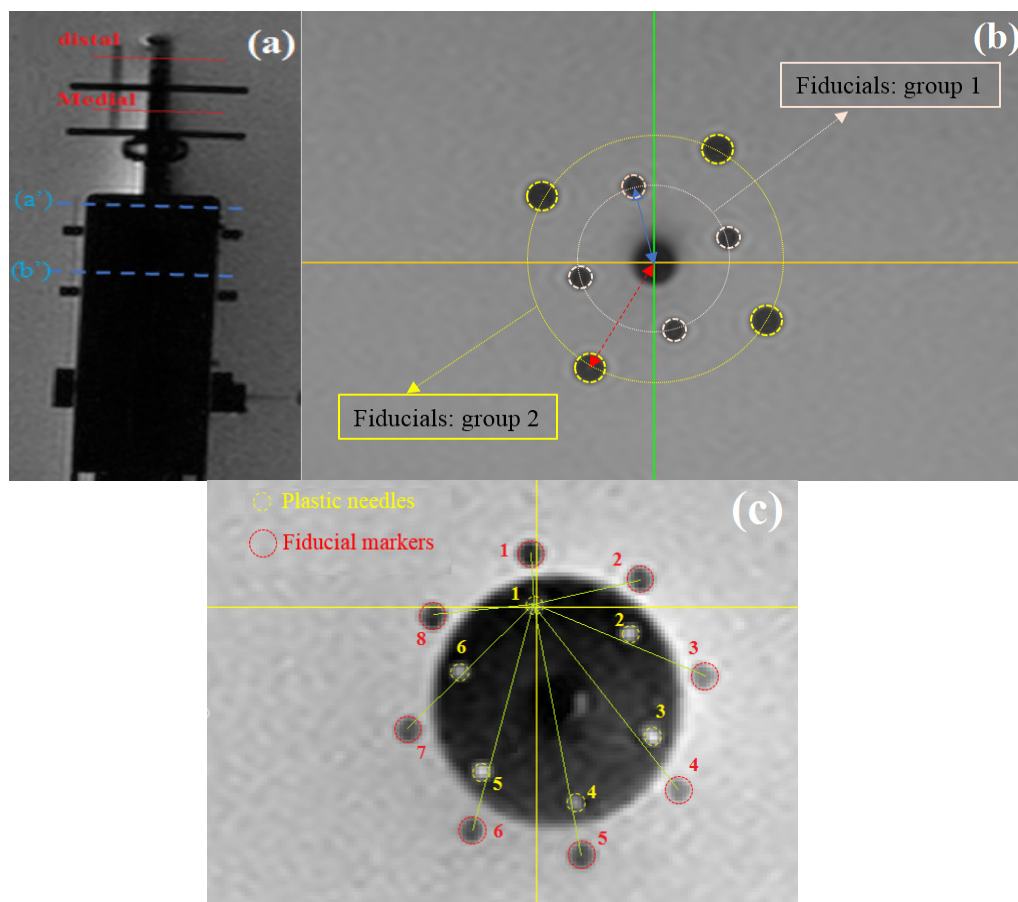


**Figure 2:** T2-weighted magnetic resonance (MR) images of the Portio applicator in the phantom assembly: (a) a para-sagittal view of the applicator, demonstrating axial planes for assessing artifact and distortion. (b) Para-axial image at the distal position, displaying fiducial markers groups 1 and 2. (c) para-axial image at position a', showing the six plastic channels and eight fiducial markers.

ment tool in NIH ImageJ v1.53 software (NIH ImageJ; NIH, Bethesda, MD) [21]. The analysis was conducted using Microsoft Excel to calculate averages and uncertainties. A similar approach was applied for the cylinder and plastic channels, where the cylinder width was measured at two positions (a' and b') along its long axis (Figure 2(a)). The differences between each channel and the eight fiducials shown in Figure 1(d) were determined on both CT and MR images (Figure 2(c)).

### Evaluation of Susceptibility Artifacts

To assess the applicator-induced artifacts, we followed the approach described by Soliman et al. [22]. The measured applicator diameter was used to represent the artifact severity, and MR images were acquired without fiducial markers, and a different image was created by subtracting the image with the applicator from the image without it. The coil position on the phantom was marked to have the same coil position in all images. Two transversal slices (distal and medial) were selected in para-axial images, and four-line profiles were drawn on the different images, separated by 45° on each slice. Additionally, a slice containing the entire tandem was selected in para-sagittal and paracoronar views. Profiles were drawn perpendicular to the long axis of the tandem at distal and medial positions. Therefore, 12 profiles were plotted on three views. We measured the full width at half-maximum (FWHM) for all profiles. The same task was performed at position a' on para-axial images for the channels and the cylinder, resulting in 24 profiles for all channels and four profiles for the cylinder.

The analyses were performed using NIH ImageJ v1.53, Matlab R2017a (Mathworks®), and Origin 2019b (OriginLab Corporation, Northampton, MA, USA).

### Image Contrast and Signal-to-Noise Ratio (SNR)

Two small regions of interest (ROIs) were

placed at the previous positions in the tandem and channels in para-axial images. One ROI was located at the tandem (or channel), while the other one was positioned 1.0 cm away from the tandem/channel in the surrounding area. The ROIs were circles with diameters of 1, 0.5, and 3 mm within the tandem, channels, and surrounding region. The image contrast was calculated using the equation [23]:

$$C=(S_s-St/n)/S_s \quad (1)$$

where,  $S_s$  was the average signal in the surrounding environment of the tandem/channel, and  $St/n$  denoted the average signal within the tandem/channel.

A 300 mm<sup>2</sup> ROI was placed in a central slice within the phantom image without the applicator to determine the SNR. The ROI mean was divided by the standard deviation to calculate the SNR [23, 24]. This task was repeated three times, and all analyses were performed using ImageJ software.

### Applicator Reconstruction Accuracy

Applicator reconstruction accuracy was validated by comparing applicator reconstruction on T2W MR images and CT images using a SagiPlan treatment planning system (Eckert & Ziegler BEBIG, GmbH, Germany). Applicator reconstructions were performed using the applicator library. The difference for each dwell position (DP) was determined for the tandem and eight channels in the lateral, anterior-posterior, and cranial-caudal directions (x, y, and z, respectively). The applicator was reconstructed three times, and the mean±standard deviation was calculated for each DP.

## Results

### Applicator Visualization

Figure 3 illustrates a typical example of the Portio applicator observed on T2-weighted (T2W) images. The tandem part is distinctly visible on T2W images, exhibiting a reproducible artifact pattern at the tip (Figure 3(a)). The T2W images also provide clear visualiza-

tion of the vaginal cylinder. Additionally, a discernible signal from the channel located at the distal part of the cylinder (position a') can be observed in Figure 3(b). However, it was necessary to adjust the image display window level to construct the trajectory of each channel without the aid of MR contrast markers inside the channels (Figure 3(c)). Similarly, adjusting the image display window level was required to visualize the trajectory of the tandem inside the cylinder.

### Distortion analysis

Figure 4(a) shows the differences in distance from the tandem to the fiducial markers between CT and MR images at the distal and medial positions. The maximum differences were 0.49 and 0.39 mm at the distal and medial positions, respectively. The corresponding average differences were  $0.28 \pm 0.02$  mm and

$0.22 \pm 0.09$  mm. Figure 4(b) shows the average displacement versus the radial distance from the tandem, separately for fiducial groups 1 and 2. The average difference was 0.28 mm within a 10 mm distance from the tandem, while beyond this distance, it reduced to 0.10 mm.

Figure 5 shows the differences in distance from each plastic channel to all markers between CT and MR images. The maximum and average differences were 0.8 mm and  $0.13 \pm 0.26$  mm, respectively. The overall mean  $\pm$  standard deviation of distance difference on MR images compared to CT images for the whole applicator was less than  $0.2 \pm 0.2$  mm for T2W MR images.

### Artifact analysis

Figure 6(a) and (b) demonstrate the analysis procedure for drawing profiles and determin-

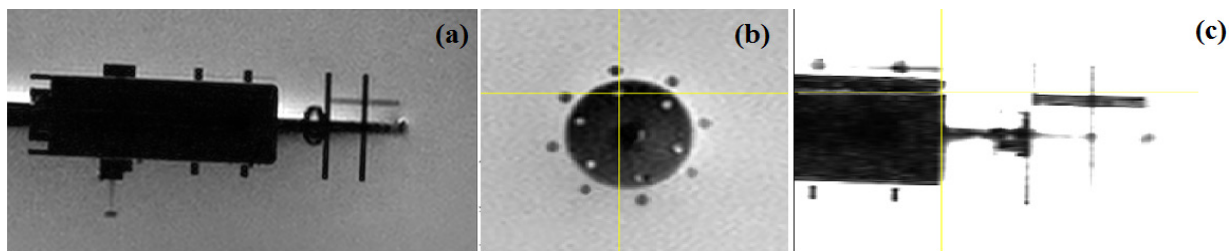


**Figure 3:** (a) A para-coronal view of the Portio applicator with the fiducials, showing the tandem and the vaginal cylinder, (b) a para-axial image at the distal position of the cylinder showing the fiducial markers and six plastic channels, and (c) the para-coronal view of the Portio applicator after adjusting the window-level for better visualization of the marked channel.

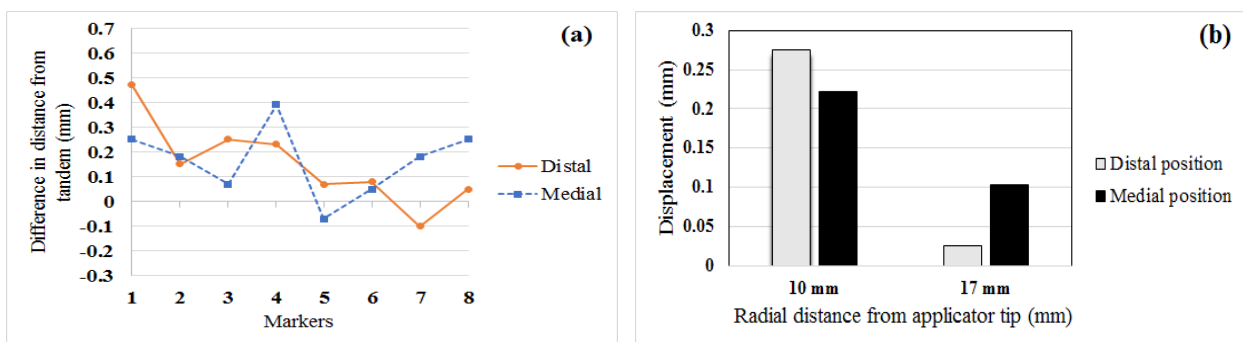


**Figure 4:** (a) The differences in distances of the fiducial markers from the tandem at the distal and medial positions (b) The displacement induced by the tandem in magnetic resonance images versus the radial distances from the tandem for distal and medial positions.

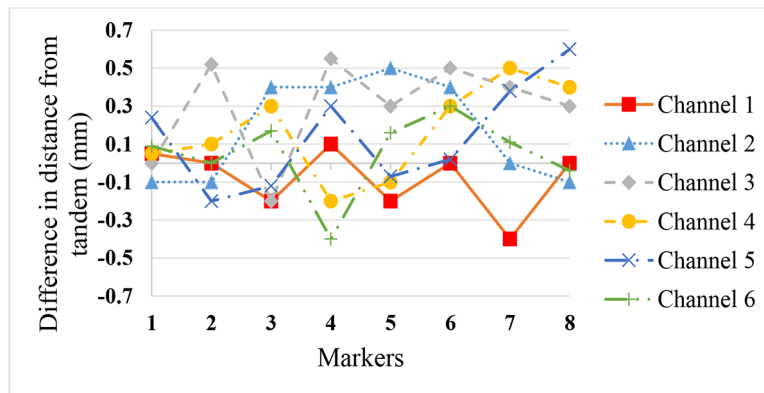


**Figure 5:** The difference in distances of the fiducial markers from each plastic channel.

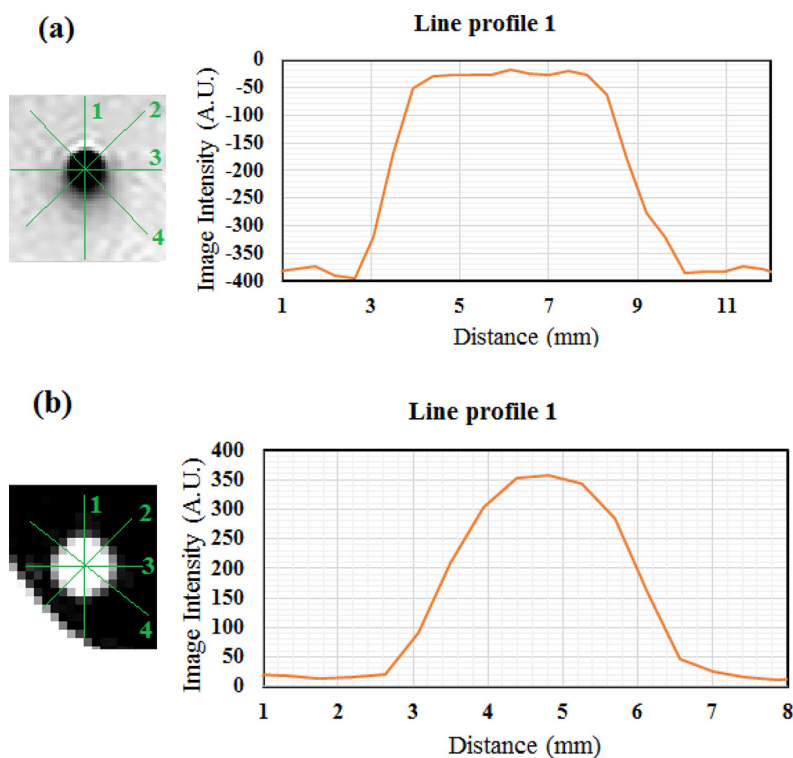


**Figure 6:** Example line profiles of the para-axial images of the (a) tandem and (b) channels.

ing FWHM for the tandem and one channel at para-axial images, respectively. FWHM measurements from the line profiles for the tandem and channels are summarized in Tables 1 and 2. The average FWHM from all profile lines from all views for the tandem was  $5.23 \pm 0.39$  mm, while the measured FWHMs were  $5.35 \pm 0.42$  mm and  $5.11 \pm 0.35$  mm for the

distal and medial positions, respectively. The average measured FWHM for all channels was  $3.21 \pm 0.37$  mm. The corresponding value for the cylinder was  $30 \pm 0.24$  mm.

#### Image contrast and SNR

The average tandem-phantom contrast was  $0.94 \pm 0.16$ , while the corresponding value for

the channels-phantom was  $0.75\pm 0.07$ . The SNR was  $73.4\pm 6.4$ .

### Applicator reconstruction accuracy

Table 3 demonstrates the average $\pm$ SD of the distance difference between CT and MRI-based applicator reconstruction for DPs. The average difference was  $0.75\pm 0.3$  mm for all DPs of the Portio applicator. The differences were  $0.71\pm 0.15$  mm and  $0.80\pm 0.70$  mm for the tandem and channels, respectively. The highest difference was found in the cranial-caudal direction.

### Discussion

Compared to CT, MRI is a well-known modality for improving target delineation. However, applicator-induced artifacts may pose a potential obstacle to applicator reconstruction and target delineation [25]. Subsequently, this may particularly affect the dose volume histograms of the organs at risk [26]. Hence, it

is crucial to evaluate the artifacts induced by new applicators introduced into a department, before clinical use [10, 11, 20]. To the best of our knowledge, the current study is the first to evaluate image characteristics of a relatively recently commercialized Portio applicator as an MCVV for 1.5 T MRI.

In this study, we evaluated image artifacts and distortions caused by the Portio applicator in a phantom environment. We also compared the reconstruction accuracy of the applicator between CT and MR-based BT. Finally, contrast and SNR were assessed for phantom images in the presence of the applicator.

We found that the total mean displacement of the whole applicator at 1.5 T was less than  $0.2\pm 0.2$  mm for T2W MR images. The extent of the distortion was not larger than the image spatial resolution ( $0.5\pm 0.5$  pixels). The maximum recorded FWHMs were  $5.40\pm 0.48$  mm and  $3.40\pm 0.27$  mm for the tandem and channels, respectively (Tables 1 and 2). This means

**Table 1:** Average full-width-at-half-maximum (FWHM) values obtained from all profile lines drawn on para-axial, para-sagittal, and para-coronal applicator images of the tandem

	Para-axial planes		Para-sagittal and para-coronal planes	
	Distal position	Medial position	Distal position	Medial position
Mean $\pm$ SD (mm)	$5.30\pm 0.37$	$5.10\pm 0.26$	$5.40\pm 0.48$	$5.12\pm 0.46$

**Table 2:** Average full-width-at-half-maximum (FWHM) values from all profile lines drawn on para-axial images of the channels

	Channels					
	1	2	3	4	5	6
Mean $\pm$ SD (mm)	$3.20\pm 0.25$	$2.96\pm 0.47$	$3.10\pm 0.36$	$3.30\pm 0.45$	$3.40\pm 0.27$	$3.30\pm 0.46$

**Table 3:** Average differences in dwell positions between computed tomography (CT) and magnetic resonance imaging (MRI)-based reconstruction for lateral (x), anterior-posterior (y), and cranial-caudal (z) directions

	Tandem			Channels			Overall		
	x	y	Z	x	y	z	x	y	z
Mean $\pm$ SD (mm)	$0.70\pm 0.10$	$0.54\pm 0.21$	$0.92\pm 0.12$	$0.98\pm 0.70$	$0.38\pm 0.75$	$1.00\pm 0.70$	$0.85\pm 0.68$	$0.45\pm 0.70$	$0.95\pm 0.60$

that the maximum artifact levels were  $0.9 \pm 1.1$  pixels and  $0.9 \pm 0.6$  pixels for the tandem and channels when using T2W MRI. Therefore, this suggests that this applicator may be used in an MR-only workflow, to avoid the registration errors caused by the MR-CT registration process [27, 28]. We expect any negative implications of MRI-based BT for the Portio applicator will be limited since the distortions and artifacts found in the present study were less than 1 mm [26]. Although distortion levels will be higher for the 3T MR images, it is expected that they will be acceptable for MRI-based BT [28].

The comparative analysis showed that the difference between CT-based and MRI-based reconstruction for the Portio applicator was within 1 mm. This small difference can result in a difference of less than 5% for the  $D_{2cc}$  of the rectum and bladder, as well as less than 2% for  $D_{90}$  of the gross tumor volume [26]. Therefore, it is not likely to significantly impact the dose distribution for organ-at-risk or the target volume. Moreover, the overall geometric accuracy of the treatment depends on both the applicator reconstruction accuracy and the volume delineation accuracy. Since MRI improves the soft tissue contrast and reduces contouring uncertainty, the most significant component in BT [29], this decrease in the accuracy of applicator reconstruction in MRI than CT does not result in a deterioration in the overall geometric accuracy [30].

The SNR and contrast values measured in our study are comparable to standard images from other BT applicators [23, 31]. However, it needs a further clinical study to assess image quality for patients. We implemented a body coil for acquiring MR images to enhance the SNR. However, we marked the coil position on the phantom to ensure that the coil position was the same between the scans with and without the applicator. Therefore, we minimized intensity variations caused by the coil, without lowering SNR [22].

Meanwhile, this study has some limitations.

First, it is a phantom-based, pre-clinical investigation, and further clinical evaluation using MR images of patients with the Portio applicator is needed. However, this study can be a foundation for future clinical studies. Second, artifacts and distortions were only evaluated using one configuration of this applicator. Different applicator configurations with different diameters and angles of the tandem, as well as different diameters of the cylinder, might result in different artifacts and distortions. However, susceptibility artifacts are likely to have a lower impact on treatment uncertainty than contouring and patient movement uncertainties [29].

Furthermore, the implemented approach does not consider out-of-plane artifacts which can extend for one or two slices away from the acquired plane [22]. We performed MR imaging with a 2 mm slice thickness to minimize this effect without lowering the SNR.

Reconstruction of the Portio applicator on the T2W sequence was performed without using the MR contrasts within the applicator and channels. We had to adjust the window level to better visualize the applicator trajectory, particularly for six channels. This required a relatively long time for the applicator reconstruction. It is reliable for the primary purpose of this study, which was to evaluate image artifacts and distortions induced by the applicator. However, the MR contrast enhancers should be used in clinical situations [20, 32]. Also, we did not use an optional cap of the applicator which can be placed at the end of the vaginal cylinder for some intrauterine tubes in the current study. We require an MR contrast enhancer for visualization of the channels' tip in the vaginal cylinder in a clinical scenario using the cap.

In this paper, we evaluated the artifacts and distortions caused by an MCV C Portio applicator at 1.5 T. Understanding the extent of the artifacts and distortions caused by a new applicator could help BT expertise for applicator reconstruction or possible strategies to reduce

severe impacts in MRI-based BT.

## Conclusion

The finding of this study showed that the levels of artifacts and distortions induced by Portio multi-channel applicator are acceptable on 1.5 T, T2W images. The maximum artifact and distortion levels were 0.9 and 0.5 pixels when using T2W MRI which were smaller than one image spatial resolution. This suggests that it can be a useful tool for MRI-based vaginal BT requiring MCVCs. However, MR contrast markers are needed for the reconstruction of the channels. Further in-patient investigation is also indicated.

## Acknowledgment

The authors would like to thank BEBIG Medical GmbH and Saman Tabesh companies as well as the staff at our Radio-oncology and MRI Departments for their help and cooperation.

## Authors' Contribution

MA. Mosleh-Shirazi and A. Kanani conceived and planned the research idea. A. Kanani performed the experimental work, wrote the manuscript, and interpreted the results with support from MA. Mosleh-Shirazi. A. Owrangi, M. Yazdi, and A. Fatemi-Ardekani verified the experimental methods and interpreted the results. H. Baghabni was a major contributor to MR imaging. All authors discussed the results, and read and approved the final version of the manuscript.

## Ethical Approval

This is a pure phantom study and no ethical approval is required.

## Funding

This work was extracted from a PhD thesis by AK, which was supported by the Vice-Chancellery of Research of our University (project number: 12353).

## Conflict of Interest

None

## References

1. Sung H, Ferlay J, Siegel RL, Laversanne M, Soerjomataram I, Jemal A, et al. Global cancer statistics 2020: GLOBOCAN estimates of incidence and mortality worldwide for 36 cancers in 185 countries. *CA Cancer J Clin.* 2021;**71**(3):209-49. doi: 10.3322/caac.21660. PubMed PMID: 33538338.
2. Nout RA, Smit V, Putter H, Jürgenliemk-Schulz IM, Jobsen J, Lutgenes L, et al. Vaginal brachytherapy versus pelvic external beam radiotherapy for patients with endometrial cancer of high-intermediate risk (PORTEC-2): an open-label, non-inferiority, randomised trial. *Lancet.* 2010;**375**(9717):816-23. doi: 10.1016/S0140-6736(09)62163-2. PubMed PMID: 20206777.
3. Nout RA, Putter H, Jürgenliemk-Schulz IM, Jobsen J, Lutgenes L, Van Der Steen-Banasik E, et al. Five-year quality of life of endometrial cancer patients treated in the randomised Post Operative Radiation Therapy in Endometrial Cancer (PORTEC-2) trial and comparison with norm data. *Eur J Cancer.* 2012;**48**(11):1638-48. doi: 10.1016/j.ejca.2011.11.014. PubMed PMID: 22176868.
4. De Boer SM, Nout RA, Jürgenliemk-Schulz IM, Jobsen J, Lutgens Ludy CHW, Van Der Steen-Banasik E, et al. Long-term impact of endometrial cancer diagnosis and treatment on health-related quality of life and cancer survivorship: results from the randomized PORTEC-2 trial. *Int J Radiat Oncol Biol Phys.* 2015;**93**(4):797-809. doi: 10.1016/j.ijrobp.2015.08.023. PubMed PMID: 26530748.
5. Viswanathan AN, Erickson BA. Three-dimensional imaging in gynecologic brachytherapy: a survey of the American Brachytherapy Society. *Int J Radiat Oncol Biol Phys.* 2010;**76**(1):104-9. doi: 10.1016/j.ijrobp.2009.01.043. PubMed PMID: 19619956.
6. Haie-Meder C, Pötter R, Van Limbergen E, Briot E, De Brabandere M, Dimopoulos J, et al. Recommendations from Gynaecological (GYN) GEC-ESTRO Working Group (I): concepts and terms in 3D image based 3D treatment planning in cervix cancer brachytherapy with emphasis on MRI assessment of GTV and CTV. *Radiother Oncol.* 2005;**74**(3):235-45. doi: 10.1016/j.radonc.2004.12.015. PubMed PMID: 15763303.
7. Pötter R, Haie-Meder C, Van Limbergen E, Barillot I, De Brabandere M, Dimopoulos J, et al. Recommendations from gynaecological (GYN) GEC ESTRO working group (II): concepts and

- terms in 3D image-based treatment planning in cervix cancer brachytherapy—3D dose volume parameters and aspects of 3D image-based anatomy, radiation physics, radiobiology. *Radiother Oncol.* 2006;**78**(1):67-77. doi: 10.1016/j.radonc.2005.11.014. PubMed PMID: 16403584.
8. Schwarz JK, Beriwal S, Esthappan J, Erickson B, Feltmate C, Fyles A, et al. Consensus statement for brachytherapy for the treatment of medically inoperable endometrial cancer. *Brachytherapy.* 2015;**14**(5):587-99. doi: 10.1016/j.brachy.2015.06.002. PubMed PMID: 26186975.
  9. Kamrava M, Leung E, Bachand F, Beriwal S, Chargini C, D'Souza D, et al. GEC-ESTRO (ACROP)–ABS–CBG consensus brachytherapy target definition guidelines for recurrent endometrial and cervical tumors in the vagina. *Int J Radiat Oncol Biol Phys.* 2023;**115**(3):654-63. doi: 10.1016/j.ijrobp.2022.09.072. PubMed PMID: 36191741.
  10. Fagerstrom JM, Kaur S. Simple phantom fabrication for MRI-based HDR brachytherapy applicator commissioning. *J Appl Clin Med Phys.* 2020;**21**(11):283-87. doi: 10.1002/acm2.13039. PubMed PMID: 33016469. PubMed PMCID: PMC7700937.
  11. Kanani A, Owrangi AM, Mosleh-Shirazi MA. Comprehensive methodology for commissioning modern 3D-image-based treatment planning systems for high dose rate gynaecological brachytherapy: A review. *Phys Med.* 2020;**77**:21-29. doi: 10.1016/j.ejmp.2020.07.031. PubMed PMID: 32768917.
  12. Glaser SM, Kim H, Beriwal S. Multi-Channel Vaginal Cylinder Brachytherapy: Impact of Tumor Size and Location on Dose to Organs at Risk. *Brachytherapy.* 2015;**14**:S78. doi: 10.1016/j.brachy.2015.08.009. PubMed PMID: 26412618.
  13. Gebhardt BJ, Vargo JA, Kim H, Houser CJ, Glaser SM, Sukumvanich P, et al. Image-based multichannel vaginal cylinder brachytherapy for the definitive treatment of gynecologic malignancies in the vagina. *Gynecol Oncol.* 2018;**150**(2):293-99. doi: 10.1016/j.ygyno.2018.06.011. PubMed PMID: 29929925. PubMed PMCID: PMC7409556.
  14. Rishi KS, David S, Pathikonda M, Ramachandra P, Giri GV, Vadaparty A, et al. Preliminary clinical outcomes of patients treated with vaginal brachytherapy alone using multi-channel vaginal brachytherapy applicator in operated early-stage endometrial cancer. *Rep Pract Oncol Radiother.* 2021;**26**(1):43-49. doi: 10.5603/RPOR.a2021.0007. PubMed PMID: 33948301. PubMed PMCID: PMC8086707.
  15. Owrangi AM, Jolly S, Balter JM, Cao Y, Maturen K, Young L, et al. Clinical implementation of MR-guided vaginal cylinder brachytherapy. *J Appl Clin Med Phys.* 2015;**16**(6):490-500. doi: 10.1120/jacmp.v16i6.5460. PubMed PMID: 26699556. PubMed PMCID: PMC5691024.
  16. Haack S, Nielsen SK, Lindegaard JC, Gelineck J, Tanderup K. Applicator reconstruction in MRI 3D image-based dose planning of brachytherapy for cervical cancer. *Radiother Oncol.* 2009;**91**(2):187-93. doi: 10.1016/j.radonc.2008.09.002. PubMed PMID: 18977049.
  17. Aubry JF, Cheung J, Morin O, Beaulieu L, Hsu IC, Pouliot J. Investigation of geometric distortions on magnetic resonance and cone beam computed tomography images used for planning and verification of high-dose rate brachytherapy cervical cancer treatment. *Brachytherapy.* 2010;**9**(3):266-73. doi: 10.1016/j.brachy.2009.09.004. PubMed PMID: 20149759.
  18. Kanani A, Owrangi A, Yazdi M, Fatemi-Ardekani A, Mosleh-Shirazi MA. Development of a multi-purpose quality control phantom for MRI-based treatment planning in high-dose-rate brachytherapy of cervical cancer. *J Contemp Brachytherapy.* 2023;**15**(1):57-68. doi: 10.5114/jcb.2023.125014. PubMed PMID: 36970435. PubMed PMCID: PMC10034728.
  19. Dimopoulos JC, Petrow P, Tanderup K, Petric P, Berger D, Kirisits C, et al. Recommendations from Gynaecological (GYN) GEC-ESTRO Working Group (IV): Basic principles and parameters for MR imaging within the frame of image based adaptive cervix cancer brachytherapy. *Radiother Oncol.* 2012;**103**(1):113-22. doi: 10.1016/j.radonc.2011.12.024. PubMed PMID: 22296748. PubMed PMCID: PMC3336085.
  20. Prisciandaro J, Zoberi J, Cohen Ga, Kim Y, Johnson P, Paulson E, et al. AAPM task group report 303 endorsed by the ABS: MRI implementation in HDR brachytherapy—Considerations from simulation to treatment. *Med Phys.* 2022;**49**(8):e983-1023. doi: 10.1002/mp.15713. PubMed PMID: 35662032.
  21. Schneider CA, Rasband WS, Eliceiri KW. NIH Image to ImageJ: 25 years of image analysis. *Nat Methods.* 2012;**9**(7):671-75. doi: 10.1038/nmeth.2089. PubMed PMID: 22930834. PubMed PMCID: PMC5554542.
  22. Soliman AS, Elzibak A, Easton H, Kim JY, Han DY, Safigholi H, et al. Quantitative MRI assessment of a novel direction modulated brachytherapy tandem applicator for cervical cancer at 1.5 T. *Radiother Oncol.* 2016;**120**(3):500-6. doi: 10.1016/j.

- radonc.2016.07.006. PubMed PMID: 27443448.
23. Rao YJ, Zoberi JE, Kadbi M, Grigsby PW, Cammin J, Mackey SL, et al. Metal artifact reduction in MRI-based cervical cancer intracavitary brachytherapy. *Phys Med Biol*. 2017;**62**(8):3011. doi: 10.1088/1361-6560/62/8/3011. PubMed PMID: 28306556.
  24. Firbank M, Coulthard A, Harrison RM, Williams ED. A comparison of two methods for measuring the signal to noise ratio on MR images. *Phys Med Biol*. 1999;**44**(12):N261-4. doi: 10.1088/0031-9155/44/12/403. PubMed PMID: 10616158.
  25. Soliman AS, Owrangi A, Ravi A, Song WY. Metal artefacts in MRI-guided brachytherapy of cervical cancer. *J Contemp Brachytherapy*. 2016;**8**(4):363-69. doi: 10.5114/jcb.2016.61817. PubMed PMID: 27648092. PubMed PMCID: PMC5018526.
  26. Tanderup K, Hellebust TP, Lang S, Granfeldt J, Potter R, Lindegaard J, et al. Consequences of random and systematic reconstruction uncertainties in 3D image based brachytherapy in cervical cancer. *Radiother Oncol*. 2008;**89**(2):156-63. doi: 10.1016/j.radonc.2008.06.010. PubMed PMID: 18692265.
  27. Krempien RC, Daeuber S, Hensley FW, Wannemacher M, Harms W. Image fusion of CT and MRI data enables improved target volume definition in 3D-brachytherapy treatment planning. *Brachytherapy*. 2003;**2**(3):164-71. doi: 10.1016/S1538-4721(03)00133-8. PubMed PMID: 15062139.
  28. Kim Y, Muruganandham M, Modrick JM, Bayouth JE. Evaluation of artifacts and distortions of titanium applicators on 3.0-Tesla MRI: feasibility of titanium applicators in MRI-guided brachytherapy for gynecological cancer. *Int J Radiat Oncol Biol Phys*. 2011;**80**(3):947-55. doi: 10.1016/j.ijrobp.2010.07.1981. PubMed PMID: 20934275.
  29. Tanderup K, Nesvacil N, Pötter R, Kirisits C. Uncertainties in image guided adaptive cervix cancer brachytherapy: impact on planning and prescription. *Radiother Oncol*. 2013;**107**(1):1-5. doi: 10.1016/j.radonc.2013.02.014. PubMed PMID: 23541642.
  30. Wills R, Lowe G, Inchley D, Anderson C, Beenstock V, Hoskin P. Applicator reconstruction for HDR cervix treatment planning using images from 0.35 T open MR scanner. *Radiother Oncol*. 2010;**94**(3):346-52. doi: 10.1016/j.radonc.2009.10.015. PubMed PMID: 19931929.
  31. Hu Y, Esthappan J, Mutic S, Richardson S, Gay HA, Schwarz JK. Improve definition of titanium tandems in MR-guided high dose rate brachytherapy for cervical cancer using proton density weighted MRI. *Radiat Oncol*. 2013;**8**:16. doi: 10.1186/1748-717X-8-16. PubMed PMID: 23327682. PubMed PMCID: PMC3556165.
  32. Sales CP, Carvalho HDA, Taverna KC, Pastorello BF, Rubo RA, Borgonovoi AF, et al. Evaluation of different magnetic resonance imaging contrast materials to be used as dummy markers in image-guided brachytherapy for gynecologic malignancies. *Radiol Bras*. 2016;**49**:165-9. doi: 10.1590/0100-3984.2015.0004. PubMed PMID: 27403016. PubMed PMCID: PMC4938446.